TRANSACTIONS ON ELECTROMAGNETIC SPECTRUM

Frequency and Time Domain Analysis of Hybrid Triple-band-notched UWB Antenna

Gabriel A. Fadehan[1], Yekeen O. Olasoji[1] and Kazeem B. Adedeji[1*]

[1]Department of Electrical and Electronics Engineering, School of Engineering and Engineering of Technology, The Federal University of Technology, Akure, Ondo State, Nigeria
Email: gabfadehan@yahoo.com, yoolasoji@futa.edu.ng, kbadedeji@futa.edu.ng

*** Corresponding author's e-mail address:** kbadedeji@futa.edu.ng

Received: 24 July 2023
Revised: 21 August 2023
Accepted: 24 August 2023

Research Article
Vol.3 / No.1 / 2024
Doi: 10.5281/zenodo.8269703

Abstract: This paper presents the analysis of a hybrid triple frequency notched ultra-wideband (UWB) antenna in the time and frequency domain. The triple-notched band was achieved by combining a modified electromagnetic band gap (MEBG) structure placed in nearness to the radiator feed and a slot element etched on the radiator. For analysis, the antenna was arranged in transmit and receive mode with a 120 mm far-field separation distance. The antenna was characterized in the frequency domain using the return loss, gain, and directivity, while the time domain focuses on the reflection coefficients at the two input ports, group delay, and fidelity factor. Less than -10 dB was achieved for the return loss. It could be observed that the received and transmitting signals are identical with fidelity of 0.992 for face-to-face and 0.928 face-to-side respectively. Also, in the frequency domain, the antenna directive gain at face-to-face and at face-to-side is given as 2.24dBi and 2.078dBi, respectively. The antenna group delay has stable characteristics in the UWB frequency band, with values less than 1 ns variation in the entire frequency band. Thus, this confirmed that the transmission performance of the antenna is linear, which is good for any applications that use UWB.

Keywords: Antenna, Band-Notch, MEBG, Fidelity Factor, Frequency Domain, Time Domain, UWB.

Cite this paper as: Fadehan GA, Olasoji YO, Adedeji KB. Frequency and Time Domain Analysis of Hybrid Triple-band-notched UWB Antenna. Transactions On Electromagnetic Spectrum 2024; 3(1): 20-33, Doi: 10.5281/zenodo.8269703

1. INTRODUCTION

Intriguing operation attributes of multiband antennas have earned important consideration in wireless communication field, where UWB systems are one of the key elements [1]. Day by day, wireless communication devices are being required to be miniaturized, more compact, and capable of accommodating end-terminal devices seamlessly [2]. In this regard, a monopole antenna is extremely used due to its lightweight, faster data rate, good precision ranging, minimal cost of production, low profile, very low spectral power density, and simplified antenna configurations that are dependable, reliable, with high system capability, to mention a few [3]. After the declaration of Federal Communication Commission rules in 2002, a variety of monopole antenna geometries have been proposed and designed so far that covers the entire band of the UWB system (3.1 GHz–10.6 GHz) over the recent years. These designs incorporate different types of patch structures and modifications; different types of ground structures and ground plane modifications; embedding of slots

and parasitic elements on the radiator; placement of different types of electromagnetic band gaps near feed lines; use of defective ground structures; and many more [4-11]. In recent years, one of the primary issues of UWB systems has been to design a system that can reduce electromagnetic interference from other narrow band radios operating within the same frequency range as the UWB system. These narrow-band communication systems include WiMAX (3.3–3.4 GHz), WLAN (5.15–5.825 GHz), INSAT (7.5–8.5 GHz), and ITU (8.01–8.5 GHz) [12–14]. Researchers have reported using a number of band stop characteristics strategies to reject some bands within the UWB system over the years [15]. These include cutting slots in the radiator surface, the ground plane, or the feed line; embedding split ring resonator (studs/knob) on the patch or the ground plane [16]; or using a complementary split ring resonator (CSSR). Parasitic elements may also be embedded in the conductor backed plane (CBP). Nevertheless, the conventional technique used in this band rejection was principally based on the employing of half-wave or quarter-wavelength filter structure in the UWB antenna [17-20].

According to research studies [21–23], frequency domain analysis is majorly studied to determine the performance and quality of UWB systems. The return loss or voltage standing wave ratio (VSWR), surface current distribution, radiation pattern, peak gain, and were principally addressed in the frequency domain. However, time domain behaviour must also be taken into account when designing an antenna for a UWB system [24]. As a result, time domain analysis helps in UWB antenna application design that can radiate short pulse signals while avoiding unwanted distortion, interference, and ringing [25]. The transient behaviour of UWB antennas is derived from their time domain analysis when operating in short pulse signals. The representation of signal distortion in relation to the radiated pulses is the major quantity of antenna transient response [26, 27]. Better energy focus property and avoidance of interference are improved with smaller time dispersion, while less stable phase centre and more interference are prominent in larger time dispersion in UWB communication with pulse radio signal [28]. The characterization of an antenna in the time domain examines the transient response of recieved signals distortion in relation to the radiated pulse signal [29]. It is an important factor that should be considered in UWB applications. The investigation therefore, should not only be performed in the frequency domain but also in the time domain. This time domain analysis the signal correlation of transmitted and received signal in an arbitrary angular direction where the pulse is preserved gives detailed characterization and determines the performance of the antenna system better than frequency domain analysis [30]. In view of this, we present the time and frequency domain analysis of a hybrid triple frequency band notch rectangular patch UWB antenna. The antenna was designed, simulated and analysed using HFSS and CST modelling tools.

2. METHODS

2.1. Triple Band Frequency Notch UWB Antenna

A triple-band frequency notch was achieved in [31] by embedding a MEBG with slot technique. The designed antenna was derived from squared radiator with both lower corner beveled to form cone shape. The dimension of the designed antenna is shown in Table 1. Frequency notching is achieved by assigning a unique band rejection frequency for each notch, while minimizing coupling effects was optimally done by positioning adjustement and shape of each element. By placing a slot on the radiator and embedding M-EBG close to the feed line, the notching was done with the goal of providing rejection for WiMAX (3.3-3.7 GHz), WLAN2 (5.15-5.825 GHz), and ITU (8.025-8.4 GHz). One slot was placed to notch the WiMAX frequency and one M-EBG embedded to notch two frequencies of WLAN and ITU as shown in Figure 1. To achieve a slot notch on the UWB patch antenna, a slot with the geometric structure shown in Figure 1(a) is cut on the radiating patch, which allows for the rejection of the WiMAX frequency band. Thereafter, M-EBG with the structure shown in Figure 1(c) was embedded on the antenna and positioned close to the feed line.

Table 1. Dimension of UWB antenna

Parameter	L	W	L1	L2	L3	L4	W1	W2
Dimension (mm)	31	24	17.7	0.5	11.5	1.5	10.25	3.3

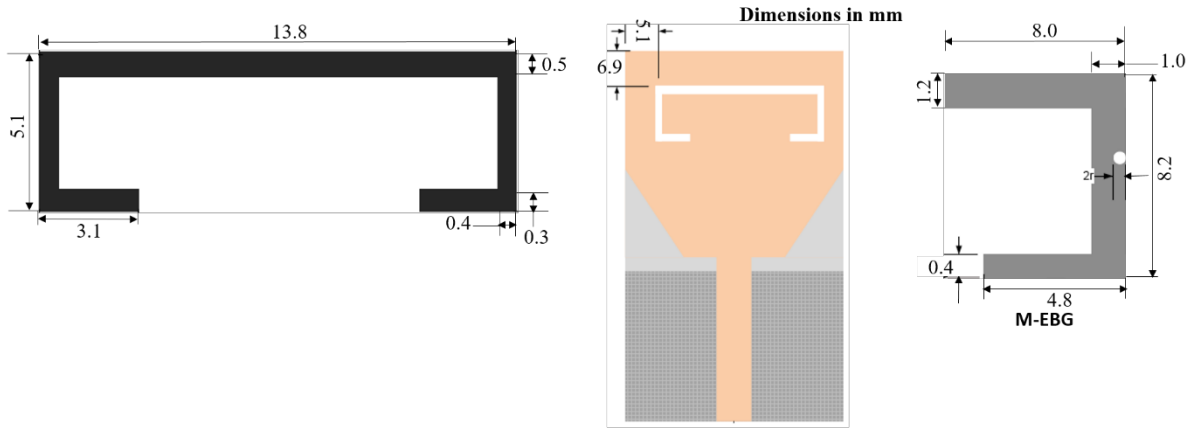

(a) (b) (c)

Figure 1. (a) Slot lay-out (b) slot position on the patch (c) M-EBG structure.

The frequency of the slot notch for narrow band frequency rejection is expressed as

$$f_{notch(slot)} = \frac{V}{2 \times l_{slot} \times \sqrt{\epsilon_{eff}}} \tag{1}$$

where v denotes light speed and l_{slot} represents the total length of the slot at needed notch band centre frequency. In Eq. (1), the effective dielectric of the slot ϵ_{effs} is expressed as

$$\epsilon_{effs} = \frac{\epsilon_r + 1}{2} \tag{2}$$

The half wavelength of the resonant frequency of the notch, f_{notch} is said to be equal to the slot length, l_{slot}. Since the slot is used to reject WiMAX frequency, therefore, using Eq. (1), at resonant frequency of WiMAX, $f_{3.54}$, the slot length is 28.8 mm. The dimensions and position of the slot on the patch antenna is shown in Figure 1(a) and Figure 1(b) respectively. The slot is positioned vertically on the radiator at 5.1 mm while the horizontal position is 6.9 mm as shown in Figure 1(b).

The M-EBG was embedded on the antenna and positioned close to the feed line. By modifying an EBG structure, an M-EBG is formed. An EBG is established by placing a structure close to a patch to produce a field gap through the ground. The ground plane is joined to the EBG structure through the via. M-EBG connected to the ground through via could be represented with approximated LC resonator circuit. The inductive (L_{in}) and capacitive (C) parts are described by Eqs. (3) to (5).

$$L_{in} = 0.20h\left[\ln\left(\frac{2h}{r}\right) - 0.750\right] \tag{3}$$

$$C = \varepsilon_0 \, \varepsilon_r \frac{w^2}{h} \tag{4}$$

$$w_0 = \frac{1}{\sqrt{L_{in} \, C}} \tag{5}$$

In Eqs. (3) to (5), ε_0 and ε_r denote absolute and relative permittivity of the material, whereas h and r indicate the via's height and radius. Similarly, w_0 and w represent the resonant angular frequency and width of the EBG respectively. The geometric structure and dimensions of the M-EBG is shown in Figure 1(c). The resulting design illustrated in Figure 2 produces a UWB antenna capable of triple-band frequency notch.

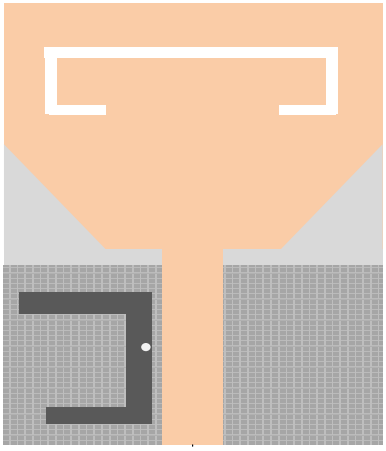

Figure 2. The hybrid triple band frequency notch UWB patch antenna.

As shown in Figure 2, the radiating part of the antenna is square-shaped, beveled at both lower corner and mounted on an FR4 substrate of 31 by 24 mm in dimensions. The UWB antenna was designed with pure copper material of 0.038mm thickness on an FR4 substrate with 4.4 dielectric constant (ϵ_r). The breadth W and length L of the patch antenna are determined using Eqs. (6) and (7) [24].

$$W = \frac{1}{2f_r\sqrt{\mu_0\epsilon_0}}\sqrt{\frac{2}{\epsilon_r+1}} = \frac{v}{2f_r}\sqrt{\frac{2}{\epsilon_r+1}} \tag{6}$$

$$L = \frac{1}{2f_r\sqrt{\epsilon_{ef}}} - 2\Delta L \tag{7}$$

where the resonant frequency of the patch is f_r, μ_0 signify the permeability in free-space, ϵ_0 represent the substrate relative permittivity, and ΔL is the extended length of the patch. In Eq. (7), the effective dielectric constant ϵ_{ef} is given as

$$\epsilon_{ef} = \frac{\epsilon_r+1}{2} + \frac{\epsilon_r-1}{2}\left[1 + 12\frac{h}{W}\right]^{-1/2} \tag{8}$$

where w and h is the dielectric substrate width and height, ϵ_r is dielectric constant of the substrate and $\frac{w}{h} \gg 1$ is the ratio of substrate width to its height. In Eq. (7), ΔL is obtained from the effective length L_{ef} for dominant mode without fringing effect as

$$L_{ef} = L + 2\Delta L \tag{9}$$

The patch antenna's resonant frequency f_r depends on both its length L and the speed of light as

$$f_r = \frac{1}{2L\sqrt{\mu_0\epsilon_0}\sqrt{\epsilon_r}} = \frac{v}{2L\sqrt{\epsilon_r}} \tag{10}$$

The performance of the designed UWB antenna was analyzed in both time and frequency domain over a dual-core computer system with HFSS and CST modeling tools.

2.2 Time and Frequency Domain Analysis

The analysis of the antenna frequency and time domain characterization was done by exciting the transmitting antenna with 5th order derivative of a Gaussian input pulse waveform signal generator in the time domain of 300ps width (duration) using Eq. (11) [32]. The antenna was simulated with Gaussian 5th order excitation signal because it power spectral density fall with the Federal Communication Commission (FCC) mask for UWB system.

$$G_5(t) = A\left(-\frac{t^5}{\sqrt{2\pi\sigma^{11}}} + \frac{10t^5}{\sqrt{2\pi\sigma^9}} + \frac{15t^5}{\sqrt{2\pi\sigma^7}}\right) e^{\left(-\frac{t^2}{2\sigma^2}\right)} \quad (11)$$

where $G_5(t)$ is the 5th order derivative of Gaussian input pulse, A is the signal amplitude, t is the time in seconds and σ is the time constant. New parameters for time domain characterization is defined through antenna fidelity factor ρ described by Eq. (12) [33-34].

$$\rho = \max_{\tau}\left(\frac{\int s_1(t)s_2(t-\tau)dt}{\sqrt{\int s_1^2(t)dt \times \sqrt{\int s_2^2(t)dt}}}\right) \quad (12)$$

where τ is a delay that could be varied in order to make numerator a maximum, $s_2(t)$ is the received signal and $s_1(t)$ is the excited/transmitted signal.

Also, the antenna is replicated into transmitting and receiving antenna and were placed in far-field distance F_f to each other with Eqs. (13) and (14).

$$v = f\lambda \quad (13)$$

$$F_f \geq \frac{2D^2}{\lambda} \quad (14)$$

In Eqs. (13) and (14), f represents the resonate frequency, λ and D represent the wavelength and the maximum dimension of the antenna respectively.

3. RESULTS AND DISCUSSION

3.1 Frequency domain behaviour

For the analysis, the triple-band antenna was arranged in transmit and receive mode. The two antennas are placed 120 mm apart for an effective far-field distance d calculated using Eq. (14). The antennas were examined in free space in two different orientations, as shown in Figure 3 and the 3-dimensional view in Figure 4. One antenna operates in transmit mode while the other is in receive mode. As illustrated in Eq. (11), the antennas were excited with a 5th order Gaussian signal [35]. The antenna arrangements were analyzed in the frequency domain to assess the S-parameter, the gain, and directivity.

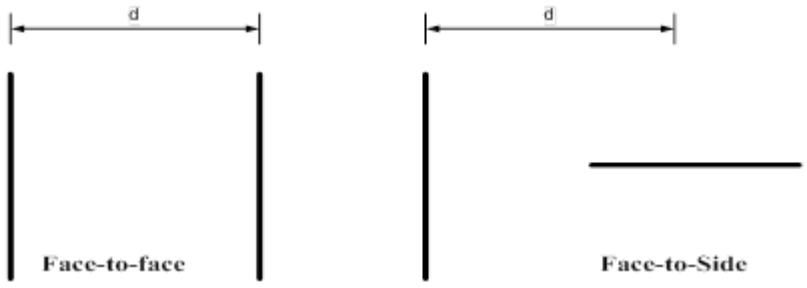

(a) (b)

Figure 3. Transmitting and receiving antenna orientation (a) face-to-face (a) face-to-side.

(a)

(b)

Figure 4. A 3D view of the transmit-receive antenna orientation (a) face-to-face (b) face-to- side.

3.1.1 The S-Parameter

An antenna S-parameter is generally referred to as return loss, and it is the measure of how small the return or reflection is. Figure 5 presents the profile of the S-parameter for the coupled antenna.

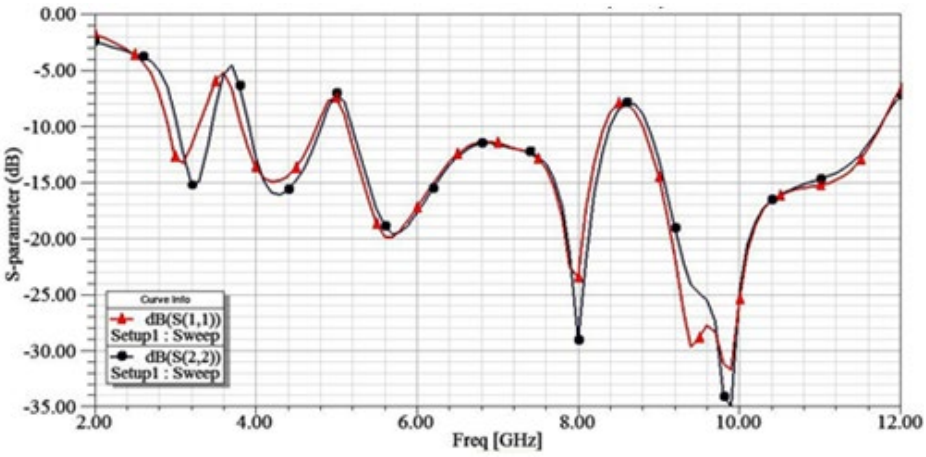

(a)

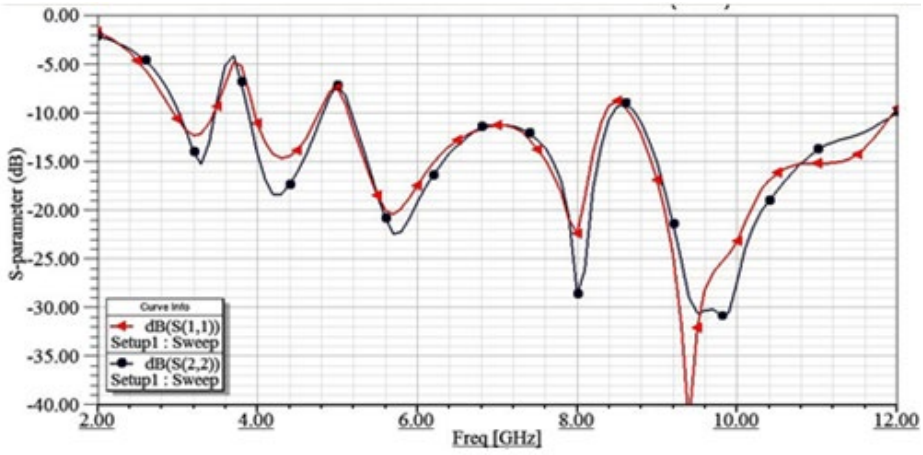

(b)

Figure 5. Transmit/receive antenna S-parameter (S_{11} and S_{22}) (a) face-to-face orientation, (b) face-to-side orientation.

It is important to mention that a coupled antenna in transmit/receive mode has more than one S-parameter. As shown in Figure 5(a), S_{11} and S_{22} has a return loss below -10dB in all UWB operating frequencies except the frequencies band corresponding to WiMAX, WLAN and ITU at face-to-face orientation. The same result was observed when the face-to-side orientation was considered in Figure 5(b). S_{11} and S_{22} are the reflection coefficients at antenna ports 1 (transmitting) and 2 (receiving) respectively. Thus, the hybrid triple band notch achieved a desirable return loss in both orientations.

3.1.2 The gain and directivity assessment

The 3-D polar plot of the antenna in transmit and receive mode is shown in Figure 6. The maximum antenna gain value averaged at 2.471dBi face-to-face and face-to-side over the range of the UWB band. Table 2 relays the detailed values of the antenna gain at different selected operating frequencies for the two orientations. When considered along with the frequency shown, the gain decreases but the latter increases as the frequency of operation increases. When considered along with antenna orientations, it could be seen that the face-to-face orientation gave a relatively better and slightly more stable antenna gain than face-to-side orientation. Nevertheless, the results show that the antenna could perform excellently at all frequencies of operation, regardless of the orientation.

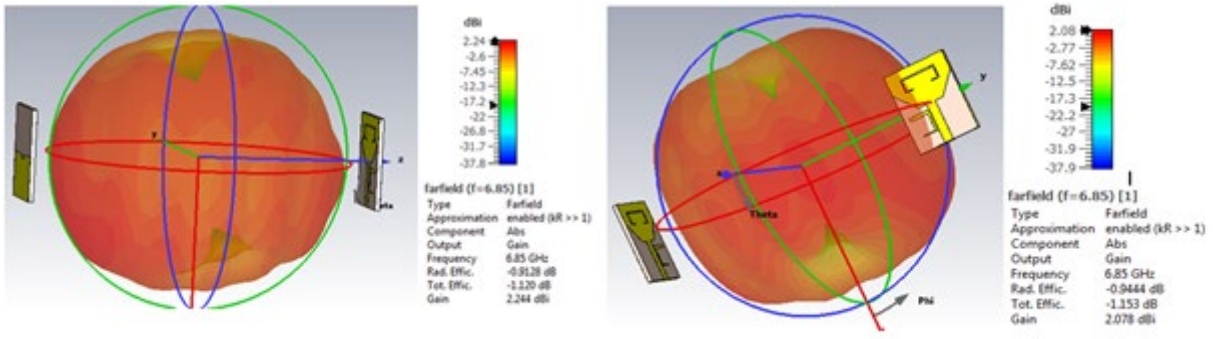

(a) (b)

Figure 6. The 3-D polar plot of transmit and receive antenna (a) face-to-face (b) face-to-side.

Table 2. Antenna gain over selected UWB frequency with face-to-face and face-to-side orientation.

Frequency (GHz)	3.1	4.5	6.85	7.5	8.5	9.5	10.2
Face-to-face (dBi)	2.92	2.085	2.224	1.758	2.649	2.707	3.678
Face-to-side (dBi)	3.119	2.437	2.079	1.878	2.705	2.13	2.231

3.1.3 Surface current distribution

The surface current distribution was shown in Figure 7. At the notch slot and EBG, the current distribution was uniform over all the selected resonant frequency. However, on the notching elements of slot and EBG, the surface current concentrations were observed. The antenna surface current gave a uniform current distribution on the patch in UWB frequency range as seen in Figure 7(a) to 7(f).

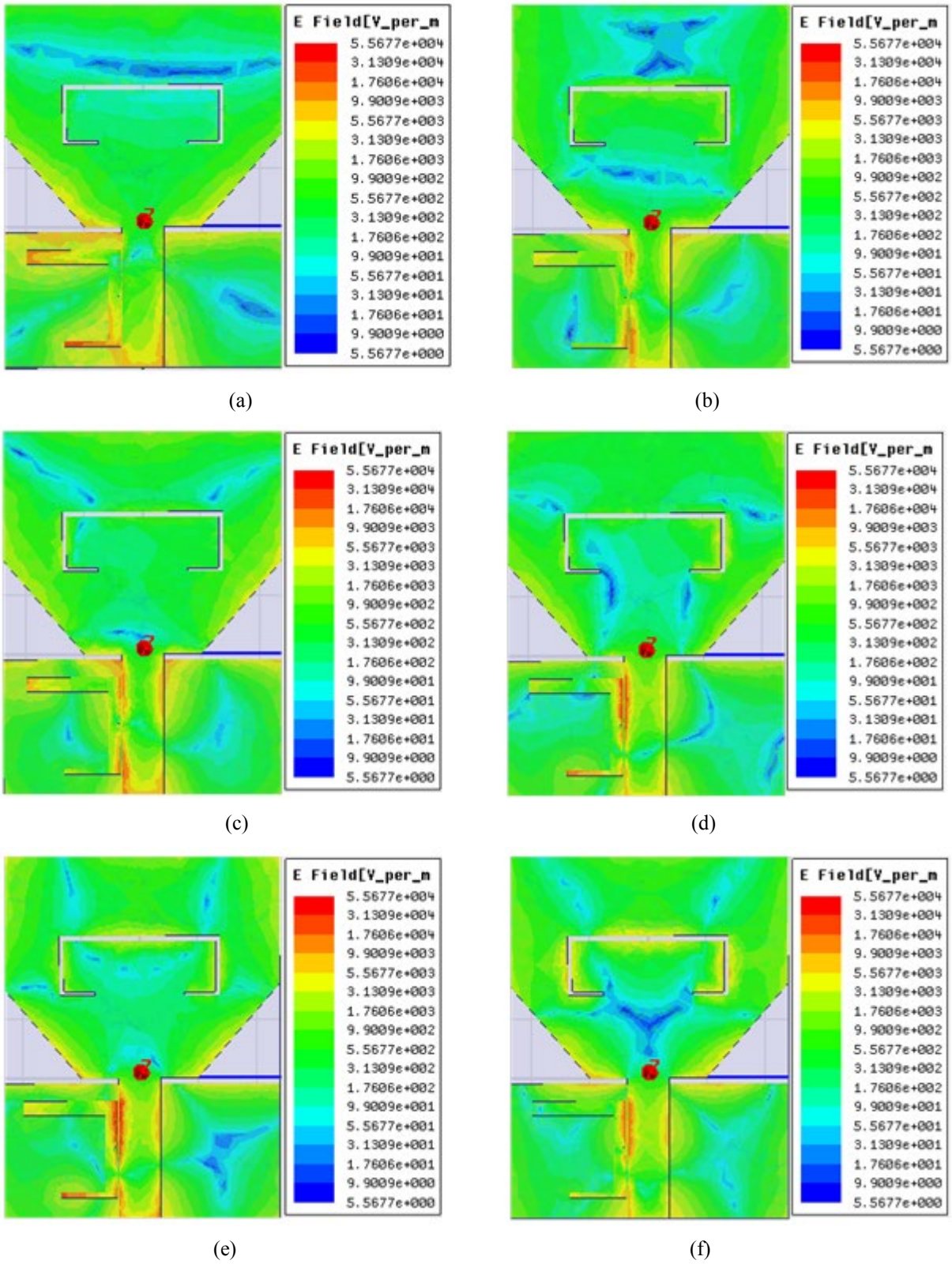

Figure 7. Surface current distribution of the designed triple-band antenna at different operating frequency (a) 4.5 GHz, (b) 6.85 GHz, (c) 7.5 GHz, (d) 8.5 GHz, (e) 9.5 GHz, (f) 10.2 GHz.

3.2 Time domain behavior

The time domain behavior includes assessing the group delay and fidelity factor of the antenna. The fidelity factor is based on the S-parameter of the transmit and receive antenna excited with a 5th order Gaussian pulse signal. The maximum correlation coefficient of the two signals when time delay τ, is varied is known as fidelity

(ρ). Fidelity gives the relationship between the transmitted pulse and received pulse with a value range from zero to unity [36]. It is a well-defined parameter used to judge the similarity of a received signal waveform with respect to the input signal as specified in Eq. (12). A fidelity factor lies between 0 and 1. A unity value means the antenna system does not distort at the input signal of the receiving antenna, where a zero value means the received signal is completely different from the transmitted signal due to attenuation. A fidelity factor of less than 0.5 completely becomes unrecognized.

3.2.1 Group delay analysis

To analyze the characteristic of the designed antenna in time domain, the antenna was excited with Gaussian signal excitation as indicated in Eq. (11). Short-duration pulses in the order of picoseconds are used for the time domain analysis to give distortion-less transmission needed for constant group delay analysis. Group delay behavior of the antenna is presented in Figure 8. The antenna group delay is the negative derivative of the phase response with respect to frequency. Group delay shows the time delay of an impulse signal at different frequencies [37]. The results demonstrated that the designed antenna has good linear transmission performance, which is good for any applications that use UWB. Likewise, the group delay has stable characteristics with values less than 1 ns variation in the whole UWB frequency band except frequencies equivalent to WiMAX, WLAN, and ITU that were notched is where the group delay variation becomes large.

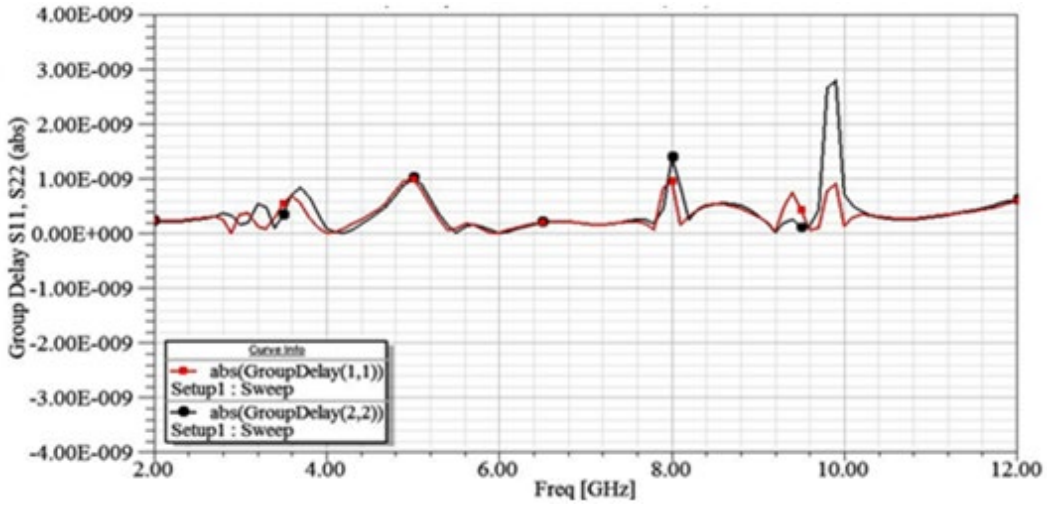

(a)

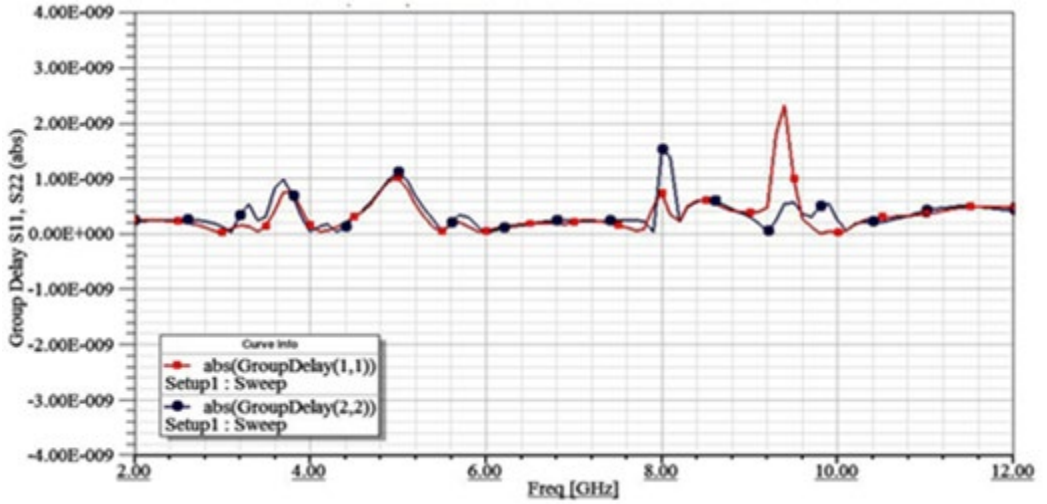

(b)

Figure 8. Group delay of transmitting and receiving antenna (a) face-to-face (b) face-to-side.

3.2.2 The fidelity factor analysis

For comparison, the fidelity factor was analyzed from the S-parameter of both orientations with Gaussian excitation at the transmit antenna and response at the receiving antenna. Some forms of distortion of the transmitted signal were expected due to notched elements. The antenna in both planes exhibits similar results. The amplitude of the received signal was low due to free-space loss, and the amplitude had to be multiplied by 5 to boost the output, as shown in Figure 9 for both orientations. The estimated S-parameter from both antennas (TX and RX) at two different orientations shows a close relationship in their path at permitted frequencies as well as a notch frequency as represented in Figure 5. The S-parameter extracted from the antenna in transmit and receive mode at two different orientations (face-to-face and face-to-side) was used in MATLAB to compute the fidelity factor expressed in Eq. (12). The fidelity between transmitted and received signals shows close value for the two antennas at face-to-face and at face-to-side. As shown in Table 3, fidelity factor of 0.992 and 0.928 was obtained for face-to-face and face-to-side respectively. The results obtained show that the antenna has an excellent fidelity factor in both orientations. Thus, in an antenna array system, the best option is to position the antenna face-to-face as it has the best fidelity factor.

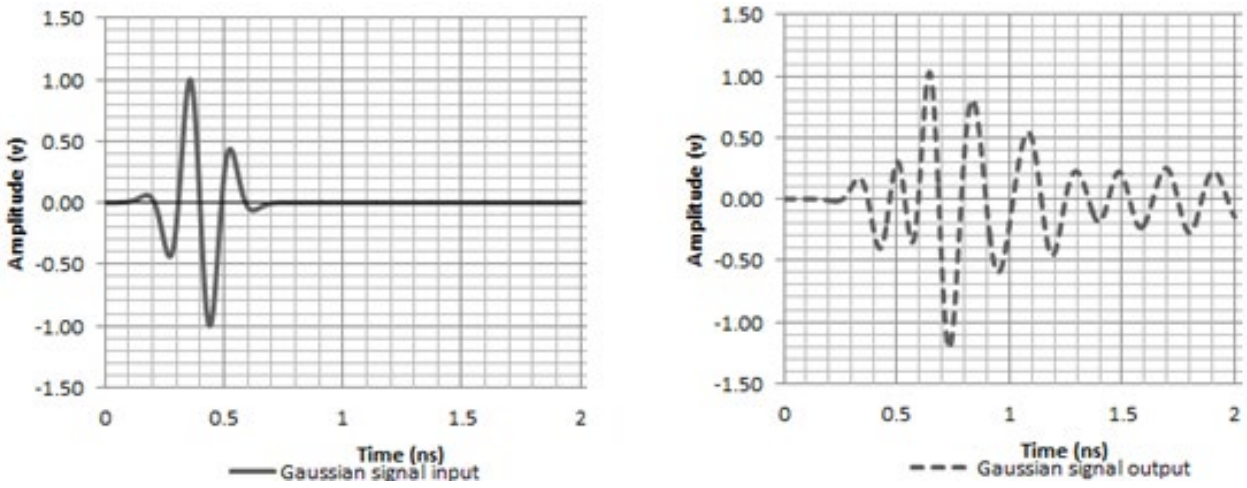

(a) (b)

Figure 9. Signal excitation of the antenna (a) input (b) output.

Table 3. The triple band notch UWB antenna fidelity factor.

Antenna orientation	Fidelity factor
Face-to-face	0.992
Face-to-side	0.928

Table 4 gives a comparison of the designed antenna with previously reported works in the literatures. The comparison comprises of time domain parameters in terms of correlation while the frequency analysis shows the impedance bandwidth of the design.

Table 4. Comparison of UWB antennas in terms of their frequency and time domain analysis.

Study	Antenna type and Design	Correlation	Notched frequencies	Impedance Bandwidth
[38]	An arrow shaped patch antenna (30 × 30 mm) with truncated ground plane utilized separated slit pair on the radiator to obtain dual notched frequency	F2F: 0.6315 S2S: 0.7914	3.3–3.9 GHz 5.1–5.9 GHz	2.2–11 GHz.
[39]	A compact tri-band notched was achieved with modification of radiating element and DGS techniques used for high impedance bandwidth	NA	3.3-3.7 GHz 5-6 GHz 7.1-7.76 GHz	2.38-2.46, 3.1-11 GHz
[40]	A modified Vivaldi antenna (50 × 50 mm.) was designed and optimized by adding corrugation on the edge of exponential flaring and grating elements on the slot area.	0.9	NA	3.1–10.6 GHz
[41]	A step slotted patch. Of 20 X 20 mm diameter applicable for WLAN and WiMAX were designed. Split patched technique was used to overcome narrow bandwidth and achieved wide bandwidth	NA	NIL	4.3–6.45 GHz
[42]	Resistive and reactive loading network combined with Pulse matching tapered slot line antenna (PMA).	NA	NIL	4 - 10 GHz.
[43]	A reconfigurable patch antenna with switchable frequency notched designed. Notching was achieved with two parasitic elements attached to the two sides of the patch while PIN diodes were placed at appropriate places on the patch for achieving four frequencies notch.	NA	3.1–13 GHz 5.1–5.7 GHz 7.2–7.8 GHz	3.1–13 GHz
This study	A Modified EBG and single slot element were used with beveled rectangular radiating patch for tri-band frequency notching.	F2F:0.992; F2S: 0.928	6.85 GHz	3.1 – 12.3 GHz

4. CONCLUSIONS

In this paper, a hybrid triple-notch-band frequency UWB antenna analyzed in both the main (frequency) and temporal (time) domain behavior was presented. The antenna was paired in transmit and receive mode with an effective far field distance to investigate its characterization both in the frequency and time domain. A Gaussian pulse signal was used for the antenna excitation of short pulses in the order of picoseconds while group delay and correlation were investigated for time domain analysis, while the impedance bandwidth, directivity, gain and surface current distribution give the frequency domain analysis of the designed antenna. It could be inferred that the received signal is identical to the transmitted signal, as seen in the fidelity factor for face-to-face and face-to-side 0.992 and 0.928, respectively. Also, in the frequency domain, the antenna directive gain at face-to-face and at face-to-side is given as 2.24dBi and 2.078dBi, respectively. The results obtained show that the antenna has an excellent fidelity factor in both orientations. Nevertheless, in an antenna array system, the best option is to position the antenna face-to-face as it produces an excellent result in terms of the fidelity factor and the directive gain.

Acknowledgment

The management of the Federal University of Technology, Akure, were healthful appreciated by the authors for the opportunity given to conduct this research.

REFERENCES

[1] Jin Y, Tak J, Choi J. Quadruple band-notched trapezoid UWB antenna with reduced gains in notch bands. Journal of electromagnetic engineering and science. 2016;16(1):35-43.

[2] Kheir M. UWB Technology: Circuits and Systems: BoD–Books on Demand; 2020.

[3] Charlier M, Koutsiamanis R-A, Quoitin B. Scheduling UWB Ranging and Backbone Communications in a Pure Wireless Indoor Positioning System. IoT. 2022;3(1):219-58.

[4] Kadu MB, Rayavarapu N. Compact stack EBG structure for enhanced isolation between stack patch antenna array elements for MIMO application. International Journal of Microwave and Wireless Technologies. 2021;13(8):817-25.

[5] Fadehan G, Adedeji KB, Olasoji YO. Parametric study and analysis of modified electromagnetic band gap in frequency notching of ultra-wide band antenna. International Journal of Engineering Research in Africa. 2022;61:151-64.

[6] Kaur K, Sivia JS, Gupta D. Microstrip Patch Antenna with Defected Ground for L, S and C Band Applications. International Journal of Computer Science and Information Security. 2017;15(2):172.

[7] Ahmad S, Ijaz U, Naseer S, Ghaffar A, Qasim MA, Abrar F, et al. A jug-shaped CPW-fed ultra-wideband printed monopole antenna for wireless communications networks. Applied Sciences. 2022;12(2):821.

[8] Jaglan N, Dalal P, Gupta SD, Abdalla MA. Band notched UWB MIMO/diversity antenna design with inductance boosted compact EBG structures. 2020.

[9] Alharbi AG, Rafique U, Ullah S, Khan S, Abbas SM, Ali EM, et al. Novel MIMO antenna system for ultra wideband applications. Applied Sciences. 2022;12(7):3684.

[10] Modak S, Daasari S, Shome PP, Khan T. Switchable/tunable band-notched characteristics in UWB and UWB-MIMO antennas: A comprehensive review. Wireless Personal Communications. 2023;128(3):2131-54.

[11] Sharma M, Singh S, Varma R. Computational design, analysis and characterization of beetle shaped high isolation multiple-input-multiple-output reconfigurable monopole-antenna with dual band filters for wireless applications. Wireless Personal Communications. 2021;119(2):1029-49.

[12] Ghosh A, Mandal T, Das S. Design and analysis of triple notch ultrawideband antenna using single slotted electromagnetic bandgap inspired structure. Journal of Electromagnetic Waves and Applications. 2019;33(11):1391-405.

[13] Doddipalli S, Kothari A. Compact UWB antenna with integrated triple notch bands for WBAN applications. IEEE access. 2018;7:183-90.

[14] Kim H, Yeon K, Kim W, Park CS. Design and implementation of electromagnetic band-gap embedded antenna for vehicle-to-everything communications in vehicular systems. ETRI Journal. 2019;41(6):731-8.

[15] Ghimire J, Choi D-Y. Design of a compact ultrawideband U-shaped slot etched on a circular patch antenna with notch band characteristics for ultrawideband applications. International Journal of Antennas and Propagation. 2019;2019.

[16] Ali EM, Awan WA, Alzaidi MS, Alzahrani A, Elkamchouchi DH, Falcone F, et al. A shorted stub loaded UWB flexible antenna for small IoT devices. Sensors. 2023;23(2):748.

[17] Zhang H, Cao X, editors. Design of quintuple band-notched UWB antenna with copper coin shaped structure. Journal of Physics: Conference Series; 2021: IOP Publishing.

[18] Abbas A, Hussain N, Lee J, Park SG, Kim N. Triple rectangular notch UWB antenna using EBG and SRR. IEEE Access. 2020;9:2508-15.

[19] Kamil AQ. Design ultra-wideband antenna have a band rejection desired to avoid interference from existing bands. Bulletin of Electrical Engineering and Informatics. 2022;11(2):886-92.

[20] Awan WA, Zaidi A, Hussain M, Hussain N, Syed I. The design of a wideband antenna with notching characteristics for small devices using a genetic algorithm. Mathematics. 2021;9(17):2113.

[21] Zehforoosh Y, Mohammadifar M, Ebadzadeh SR. Designing four notched bands microstrip antenna for UWB applications, assessed by analytic hierarchy process method. Journal of Microwaves, Optoelectronics and Electromagnetic Applications. 2017;16:765-76.

[22] Kadam AA, Deshmukh AA. Pentagonal shaped UWB antenna loaded with slot and EBG structure for dual band notched response. Progress In Electromagnetics Research M. 2020;95:165-76.

[23] Bhatia SS, Sivia JS, Sharma N, Sharma V. Electromagnetic bandgap structure and split ring slot-based monopole antenna for ultra-wideband applications with dual band notch characteristics. Engineering Reports. 2020;2(10):e12239.

[24] Pancera E, Zwick T, Wiesbeck W. Spherical fidelity patterns of UWB antennas. IEEE Transactions on Antennas and Propagation. 2011;59(6):2111-9.

[25] Yang Y, Wang B-Z, Ding S. Performance comparison with different antenna properties in time reversal ultra-wideband communications for sensor system applications. Sensors. 2017;18(1):88.

[26] Abdalla MA, Al-Mohamadi AA, Mohamed IS. A miniaturized dual band EBG unit cell for UWB antennas with high selective notching. International Journal of Microwave and Wireless Technologies. 2019;11(10):1035-43.

[27] Kumar P, MM MP, Kumar P, Ali T, Alsath MGN, Suresh V. Characteristics Mode Analysis-Inspired Compact UWB Antenna with WLAN and X-Band Notch Features for Wireless Applications. Journal of Sensor and Actuator Networks. 2023;12(3):37.

[28] Sanmugasundaram R, Somasundaram N, Rajkumar R. Ultrawideband notch antenna with EBG structures for WiMAX and satellite application. Progress In Electromagnetics Research Letters. 2020;91:25-32.

[29] Sethi D, Yadav A, Khanna R. Dual band notched ultra wideband microstrip antenna with CSRR slot and EBG structure. International Journal of Engineering Research & Technology (IJERT). 2014;3(9):2278-0181.

[30] Van den Brande Q, Lemey S, Rogier H, Vanfleteren J, editors. Coupled half-mode cavity-backed slot antenna for IR-UWB in air-filled SIW technology. 2018 IEEE International Symposium on Antennas and Propagation & USNC/URSI National Radio Science Meeting; 2018: IEEE.

[31] Fadehan G, Olasoji YO, Adedeji KB. Development of a Triple Band Notched UWB Antenna. International Journal of Engineering Research in Africa. 2023;63:97-118.

[32] Barboza SHI, Palacio JAA, Pontes E, Kofuji ST, editors. Fifth derivative Gaussian pulse generator for UWB breast cancer detection system. 2014 IEEE International Conference on Ultra-WideBand (ICUWB); 2014: IEEE.

[33] Akhoondzadeh-Asl L, Fardis M, Abolghasemi A, Dadashzadeh GR. Frequency and time domain characteristic of a novel notch frequency UWB antenna. Progress In Electromagnetics Research. 2008;80:337-48.

[34] Mane S. Overview on Ultra-Wide Band Antennas. International Journal of Research Radicals in Multidisciplinary Fields, ISSN: 2960-043X. 2022;1(2):35-40.

[35] Dilruba Geyikoglu M. A novel UWB flexible antenna with dual notch bands for wearable biomedical devices. Analog Integrated Circuits and Signal Processing. 2023;114(3):439-50.

[36] Kumar OP, Ali T, Kumar P. A Novel Corner Etched Rectangular shaped Ultrawideband Antenna Loaded with Truncated Ground Plane for Microwave Imaging. Wireless Personal Communications. 2023;130(3):2241-59.

[37] Malik J, Patnaik A, Kartikeyan M. Compact antennas for high data rate communication: Springer; 2018.

[38] Sanyal R, Patra A, Sarkar P, Chowdhury SK. Frequency and time domain analysis of a novel UWB antenna with dual band-notched characteristics. International Journal of Microwave and Wireless Technologies. 2017;9(2):427-36.

[39] Bharti BK, Singh AK, Gangwar RP, Verma R. Frequency and time domain analysis of triple band notched UWB antenna with integrated bluetooth band. Prog Electromagn Res M. 2021;105:109-18.

[40] Çolak SA, Tokan NT. Time-domain analysis of modified Vivaldi antennas. Antennas and Wave Propagation. 2018;74945:39-55.

[41] Khangarot S, Sravan B, Aluru N, Saadh AM, Poonkuzhali R, Kumar OP, et al. A compact wideband antenna with detailed time domain analysis for wireless applications. Ain Shams Engineering Journal. 2020;11(4):1131-8.

[42] Li S, Chen H, Zhang Q, Yang M, Zhao H, Yin X. Time-domain analysis and design of pulse matching tapered slotline antenna with resistive and reactive loading network. IEEE Transactions on Antennas and Propagation. 2020;69(7):3689-99.

[43] Oraizi H, Valizade Shahmirzadi N. Frequency-and time-domain analysis of a novel UWB reconfigurable microstrip slot antenna with switchable notched bands. IET Microwaves, Antennas & Propagation. 2017;11(8):1127-32.

